WELDING RESEARCH

SUPPLEMENT TO THE *WELDING JOURNAL*, SEPTEMBER 1988

Sponsored by the American Welding Society and the Welding Research Council

Multipass, Autogenous Electron Beam Welding

Joint geometries and weld procedures are recommended for eliminating the problems associated with root spiking and variations in penetration in deep-penetrating welds

BY J. L. MURPHY, T. M. MUSTALESKI, JR., AND L. C. WATSON

ABSTRACT. A method has been developed to make narrow, deep-penetrating electron beam welds without the problems associated with root spiking. The process uses the base metal for filler metal, supplementing it with a boss on the weld joint, which is dimensioned to suit the particular weld. The weld boss is machined subsequent to welding. This development was the result of extensive work to minimize the problems of variation in penetration, root spiking and cold shuts, which can occur in single-pass electron beam welds.

Weld joint geometries and welding procedures are detailed for partial and full penetration welds. These include welds in uranium of 0.335-in. (8.5-mm) (8 passes) to 0.830-in. (21.1-mm) (22 passes) and 0.310-in. (7.9-mm) (3 passes) aluminum Alloy 5083. For the work in aluminum Alloy 5083, multipass autogenous electron beam welds are compared with gas metal arc welds and wire-fed electron beam welds. The areas of comparison include part distortion, porosity, depletion of magnesium, and mechanical properties.

KEY WORDS

Electron Beam Welding
Autogenous Welding
Multipass EB Welding
Aluminum Alloy 5083
Uranium
Deep Penetration Welds
Narrow Penetration
Filler From Base Metal
Weld Joint Boss
Wire-Fed EB Welds

Introduction

Weld penetration variations and spiking can be associated with partial penetration electron beam (EB) welds. Similar variations of beam energy transmitted through full penetration EB welds have also been reported (Refs. 1–8). Attempts to reduce the variations and spiking led to the development of multiple pass EB welds. Initial work in this area by Bradburn, *et al.* (Ref. 5), was done autogenously, but the welds were much wider than normal EB welds. Welds were made with cold wire addition at the Oak Ridge Y-12 Plant (Ref. 9) and the Rocky Flats Plant (Ref. 10). These welds retained many of the attributes associated with single-pass electron beam welds, such as low heat input and minimal distortion. Although this heat input and distortion were increased slightly, they were still substantially below the levels associated with more conventional welding processes. This development also led to the elimination of root discontinuities such as cold shuts and porosity in deep welds, as more shallow passes are less likely to produce these flaws. To successfully accomplish these welding procedures, precision equipment was developed to position and feed very small diameter (0.015- to 0.040-in./0.4- to 1.0-mm) wire in a vacuum chamber. While this development proved that the use of small weld passes could be used to eliminate discontinuities, the necessary equipment

J. L. MURPHY, T. M. MUSTALESKI, JR., and L. C. WATSON are with the Oak Ridge Y-12 Plant, Development Division, Martin Marietta Energy Systems, Inc., Oak Ridge, Tenn.

Paper presented at the 67th Annual AWS Convention, held April 13–18, 1986, in Atlanta, Ga.

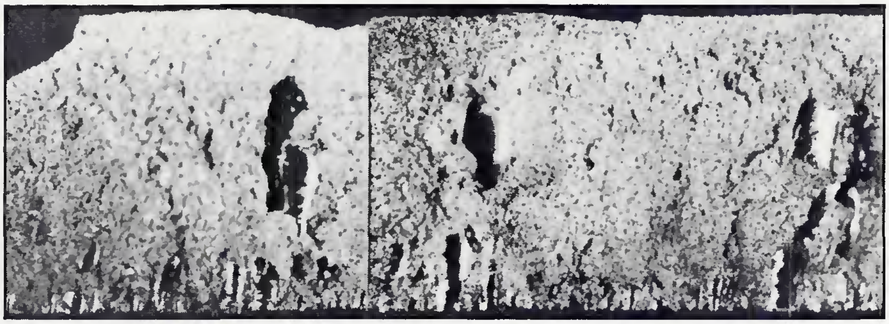

Fig. 1 — Cold shuts, up to 0.300-in. depth, in the fracture surface of a 0.650-in. deep single-pass, autogenous EBW in uranium (2X)

Fig. 2 — Longitudinal section to weld centerline of 81% penetration, single-pass, autogenous EBW in 0.340-in. wall thickness uranium (3X)

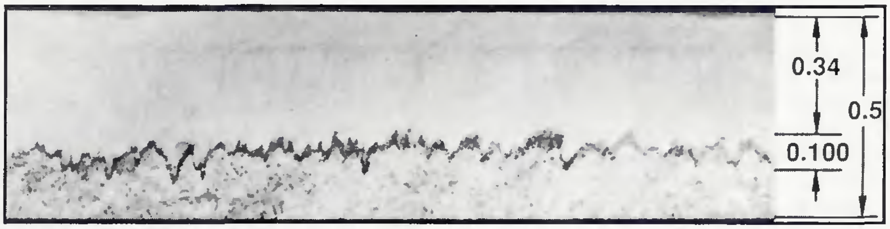

Fig. 3 — Longitudinal section to weld centerline showing "spiking" in single-pass, autogenous EBW in uranium (Dimensions in in.) (2X)

was complex and the very small diameter wire often proved difficult to fabricate and feed.

A program was, therefore, initiated to produce multipass EB welds autogenously while retaining the low heat inputs, and resultant low distortion, produced in the narrow wire-fed welds. It has been observed during wire-fed welding that some of the filler metal was being obtained from the joint sidewalls. It was hoped that a process could be developed that would exploit this phenomenon by using only the joint sidewalls for filler metal. The reduction in the joint width due to the shrinkage of each pass would continue to make additional material available. A weld boss could be added for later removal so that the weld could be filled to the part surface. The initial weld development was done using uranium because its fluidity made it suitable for multipass welding. From the work on uranium, the program was broadened to include multipass autogenous EB welding of aluminum alloys, especially the 5083 alloy. Aluminum is a more difficult material to weld than uranium, but provided a good material for comparative evaluation of this process against other welding processes.

Equipment

The equipment used for the development of this welding process was a Hamilton Standard W-2 electron beam weld machine that had been modified for computer control and wire feeding (Ref. 9). The weld machine has a maximum operating voltage of 150 kV with a maximum beam current of 40 mA, giving a maximum output power of 6.0 kW. The equipment was operated in the high-vacuum mode (vacuum of 1×10^{-4} torr or better), although it is equipped with an extended column, which would allow operation in the partial-vacuum mode. The machine has been modified to use either the R40A electron gun with a hairpin filament or the R167 electron gun with a ribbon filament. Except for the initial uranium test cylinders, all the welds for this investigation were made using the ribbon filament.

Process Development

Uranium

High depth-to-width ratio single-pass EB welds in uranium that exceed 0.2-in. (5-mm) penetration often contain weld discontinuities such as cold shuts (Figs. 1 and 2), root spiking (Figs. 2 and 3), and lack of consistent weld penetration (Figs. 2 and 3). Several authors have reported attempts to reduce the incidence of spiking and cold shuts in uranium (Refs. 4, 5, 9, 11). The first three references deal primarily with attempts to control penetration in uranium welds. Armstrong (Ref. 4) noted that the occurrence of cold shuts increased as the electron beam was defocused in an effort to reduce root spiking. Wood and Mara (Ref. 11) used alloying shims to reduce the solidification temperature of the weld pool. This technique did eliminate the cold shuts in the welds, but as will be shown, it had a significant negative effect on the fracture toughness of the weld metal. The work with the alloy additions offered no advantage in controlling the weld penetration. The inconsistent weld penetration made it difficult to achieve a deep, single-pass full penetration weld with a good root contour or a partial penetration weld with closely controlled penetration. Multipass welding was, therefore, desirable because the shallow penetration of each pass minimized these problems.

From earlier work on wire-fed EB welds in uranium (Ref. 9), initial joint geometries for use in autogenous multipass electron beam welding were designed. These joint preparations produced much deeper and narrower autogenous welds than those produced by Bradburn, *et al.* (Ref. 5). Tests in weld rings of up to 0.5-in. (12.7-mm) wall thickness led to the joint geometry shown in Fig. 4. The root face of 0.030 in. (0.76 mm) was selected to allow accurate penetration control for the root pass. After the root pass has been made, it is then possible to fill the groove by defocusing the beam to a larger diameter for

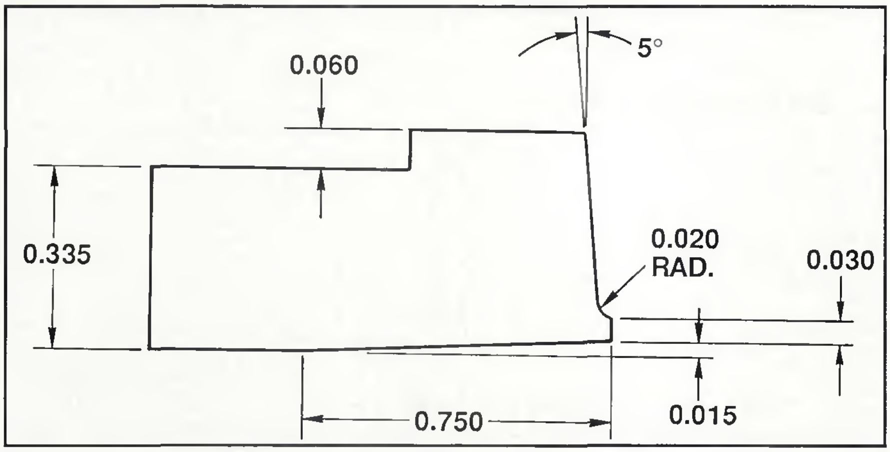

Fig. 4—Weld joint geometry for multipass, autogenous EB welding of uranium (Dimensions in in.)

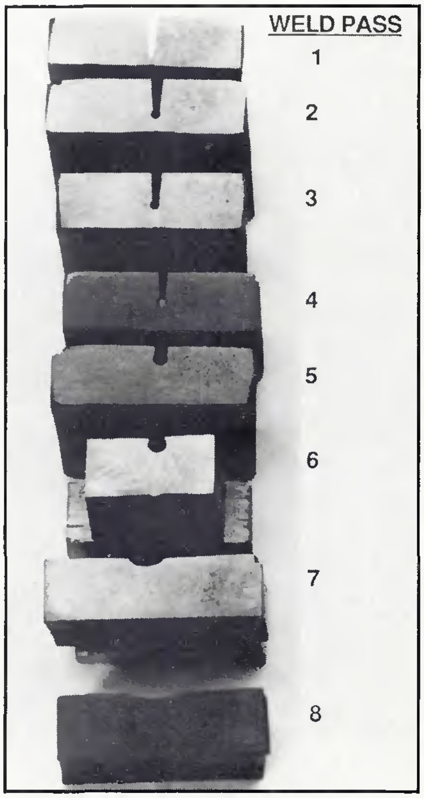

Fig. 5—Illustration of multipass, autogenous weld-joint filling of 0.395-in.-thick cast uranium (0.335-in. wall thickness and 0.060-in. weld boss)

each subsequent weld pass. The defocused beam melts metal from the groove face as well as the surface of the previous pass to create the weld. Care must be taken not to allow the metal to bridge across the groove. The progress of an 8-pass autogenous weld is shown in Fig. 5. This weld was made on a set of uranium cylinders with a 0.335-in. (8.5-mm) wall and the joint geometry shown in Fig. 4. The welding procedure used for this weld is given in Table 1. The increasing weld width as a result of the increasing beam defocus and current is evident with each weld pass. The residual underfill that is typical with these welds can be seen at the eighth pass. This depressed area is usually removed by machining after welding. The weld was made continuously with changes in the beam current and focus settings being made as each weld pass was completed.

Using this basic joint design, it was possible to increase the wall thickness to 0.5 in., plus a weld boss of 0.060 in. (1.5 mm). A weld boss of this size was found to be adequate to completely remove the weld depression in a postweld machining operation, thus leaving the entire part wall thickness intact. This total thickness of 0.560 in. (14.2 mm) was welded in 13 passes using welding parameters similar to those shown in Table 1. A weld cross-section is shown in Fig. 6. The shrinkage resulting from welds made in this manner was measured for each weld pass. A graphical representation of this shrinkage data is shown in Fig. 7. Only a few of the data points are shown so that the shape of the curve can be more readily seen. It shows that 70% of the transverse shrinkage occurs in the first five weld passes. The 13-pass weld caused a reduction of 0.045 in. (1.14 mm) in the width of the cylinders. From this data, it became evident that it would be relatively simple to modify the initial size of the parts to compensate for this shrinkage. Figure 6 illustrates the narrow weld which can be achieved with such a procedure. The excellent weld root contour shows the high quality level that can be achieved using the small root pass and an understanding of the part distortion which is caused by the multipass weld.

To further demonstrate the capability of the process, the weld shown in Fig. 8 was made. This weld was made in 0.830-in. (21.1-mm) thick beta-quenched uranium using 22 weld passes. The weld joint was similar to the one shown in Fig. 4 except for the wall thickness and the use

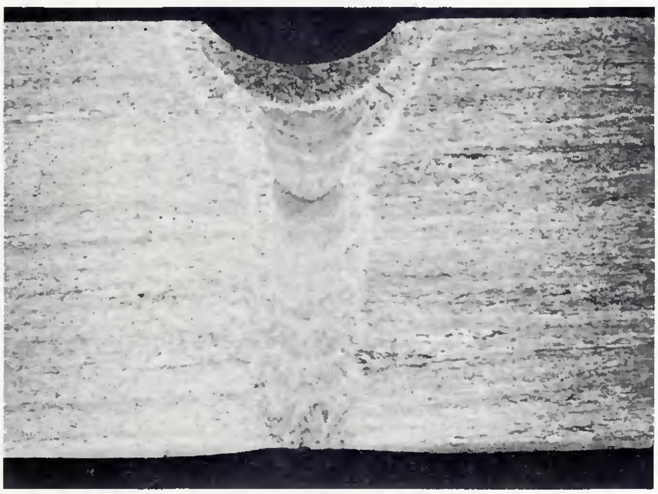

Fig. 6—Cross-section of a 13-pass, autogenous EBW in 0.560-in. thickness wrought uranium (0.500-in. wall thickness and 0.060-in. weld boss) (6X)

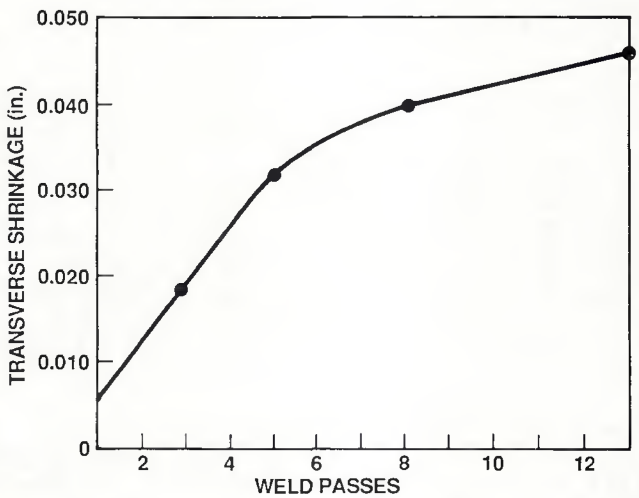

Fig. 7—Transverse shrinkage resulting from multipass weld of uranium cylinders

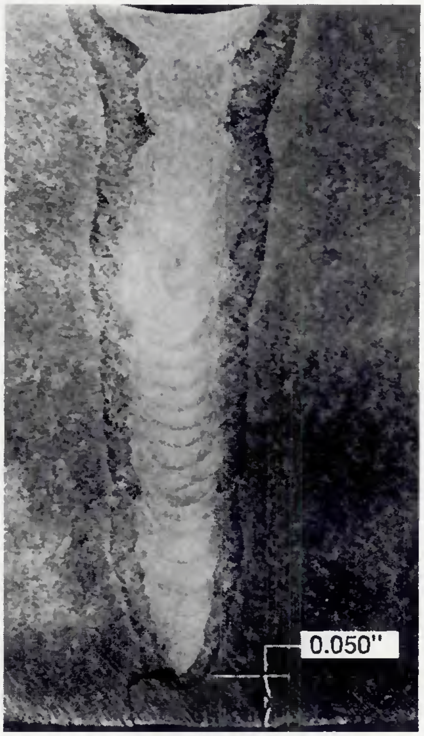

Fig. 8—93% penetration, multipass, autogenous EBW on 0.830-in.-thick beta-quenched uranium (5X)

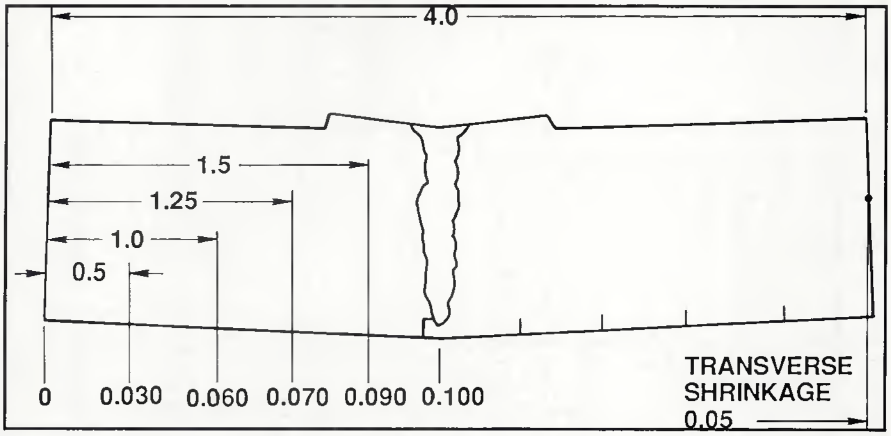

Fig. 9—Inner-contour sweep from a 93% penetration weld (a minus sign indicates radial distortion to the inside of the cylinder. Dimensions in in.)

of a 0.050-in. (1.27-mm) root face. There is also an alignment step of 0.050 in. for this partial penetration weld. The end of the step was machined to a 7.5-deg bevel angle so that the mating parts would lock together during welding. Welding parameters were similar to those shown in Table 1 except for the addition of more weld passes. The variation in weld penetration has been held to a minimum so that there is no complete penetration of the alignment step. This would have been impossible with a single-pass weld. The dimensional data taken from a set of cylinders welded with this procedure are shown in Fig. 9. The inside radius of the cylinders decreases approximately 0.10 in. (2.54 mm) immediately under the weld. The cylinders could be dimensionally compensated to correct for this distortion on both the inside and outside surfaces. This type of compensation was used for the weld shown in Fig. 6.

The welding parameters used to make the welds shown thus far were not optimized. Welds that are represented by the cross-sections shown in Figs. 5, 6 and 8 had an average fill of 0.04 in. (1.0 mm) per pass. It was of interest to reduce the number of weld passes, which in turn reduces the welding time, part distortion and the possibility for defects. A technique of oscillating the beam in the direction of welding (Y-axis) was beneficial to improving the filling of the weld.

This oscillation pattern was satisfactory because the length of the weld spot was not restrained by the weld joint. Weld fill was also improved by reducing the volume of the joint. A groove angle of 4 deg was determined by experiment to be the smallest that could be used without danger of the weld pool bridging over the joint during welding. The size of the root face also influences the number of weld passes, since fewer fill passes are needed as the root face increases. An optimized weld joint geometry is shown in Fig. 10. The root face of 0.150 in. (3.8 mm) was selected as the largest that could be used with no possibility of cold shuts. This also produced a root bead which would not penetrate the thin alignment step. Longitudinal oscillation of the beam also reduced weld spiking. A cross-section of the weld joint after the root pass is shown in Fig. 11 and a completed weld is shown in Fig. 12. The optimized welding

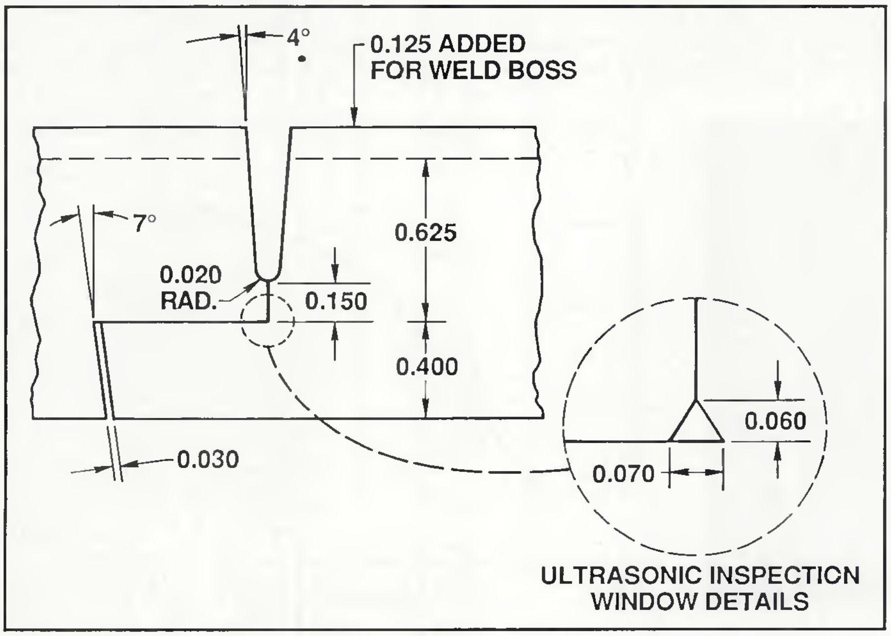

Fig. 10—Weld joint geometry for multipass, autogenous EB welding of uranium cylinders (Dimensions in in.)

Table 1—Welding Parameters for 8-Pass, Autogenous Electron Beam Weld on Uranium[a]

Weld Pass Number	Beam Current (mA)	Focus[b] (mA)
1	4.5	460
2	4.0	465
3	10.0	480
4	10.0	490
5	10.0	495
6	15.0	480
7	15.0	490
8	20.0	500[c]

(a) R-40 electron gun was used. Voltage was constant at 107 kV. Travel speed was constant at 20 ipm.
(b) A setting of 450 mA was established for a sharp focus setting at the root of the joint at a beam current value of 2 mA.
(c) The electron beam was oscillated transverse to the weld joint (X-direction) at 60 Hz and a width of 0.2 in.

Table 2—Multipass, Autogenous Electron Beam Welding Parameters

Weld Pass[a,b]	Beam Current (mA)	Beam Focus[c] (mA)	Beam Oscillation[d] (in.)
1	20	625	0.035
2	20	680	0.035
3–11	20	680	0.055
12–13	25	680	0.055
14	25	680	0.055

(a) A ribbon filament gun was used. Voltage was constant at 120 kV.
(b) Welding speed was constant at 30 ipm.
(c) Sharp focus at the root of the joint was 625 mA at a beam current value of 2 mA.
(d) The electron beam was oscillated longitudinal to the weld joint (Y-direction) at 1 kHz to the dimension shown.

Table 3—Mechanical Properties for Uranium and Uranium Welds

	Ultimate Tensile Strength (ksi)	Fracture Initiation Toughness (in.-lb/in.^{2})	Tearing Modulus (T mat)
Multipass, autogenous EBW (14 pass)[a]	123	133	33
Single-pass EBW with 0.005-in. copper shim	110	88	7
Base metal	95	152	52

(a) Beta-quenched material, all others as-rolled. All tests at 70°F.

parameters are shown in Table 2. This 19-mm weld was completed in only 14 weld passes with no parameter changes during passes 3 through 11, and only one change in the remaining passes.

Final machining of the part would remove part of the last weld bead. Distortion of weld cylinders which were 6 in. (152.4 mm) wide with an inside diameter of 14 in. (356 mm) was 0.06 in. (1.5 mm) radially inward directly under the weld.

Numerous sections were cut from cylinders that were welded with the procedure given in Table 2. These sections were bend tested to failure. Observation of the fracture surfaces revealed no cold shuts. A typical surface is shown in Fig. 13. This surface may be compared to the one shown in Fig. 1. This comparison shows that the variation in penetration and spiking are minimized (Fig. 14) even when a thick root is welded. Welds typical of the one shown in Fig. 12 contained one pore per 4 in. (100 mm) of weld length, with maximum pore diameter being 0.04 in. Typical mechanical properties for these welds, as well as single-pass welds and welds made using copper shims (Ref. 11), are given in Table 3.

Radiography cannot always detect lack of weld penetration. Shrinkage resulting from the multipass weld will force any unwelded section tightly together. Only a gross amount of incomplete penetration would be detected. Ultrasonic inspection techniques have been developed to detect incomplete penetration and the presence of cold shuts in the welds (Ref. 12). A small groove (Fig. 10) is premachined at the root of the joint. An acceptable weld would fuse the groove, resulting in a condition that would pass an ultrasonic inspection. Cold shuts in welds are detected by comparing signals produced on ultrasonic inspection equipment to the signals obtained from known standards.

Fig. 11—Cross-section from EBW on 0.150-in.-wide root face in beta-quenched uranium (5X)

Fig. 12—14-pass, autogenous, EBW in uranium (0.750 in. to the step) weld boss not removed (5X)

Aluminum Alloy 5083

In order to expand the technique of multipass autogenous EB welding to aluminum, a specification was developed for a 76% penetration weld. This specification required a minimum penetration of 0.235 in. (6.0 mm) in a pipe of aluminum Alloy 5083 with a wall of 0.310 in. (7.9 mm) without spiking through the wall. Weidner and Shuler (Ref. 7) concluded that the best penetration which could be achieved in a high-magnesium (>2.5 wt-% magnesium) aluminum alloy without spiking through was less than 75% of the wall thickness. This study also

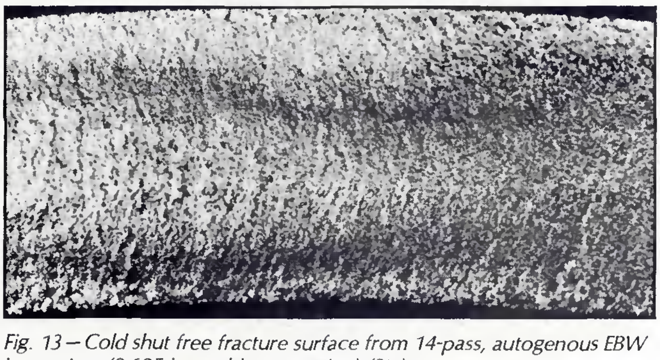

Fig. 13—Cold shut free fracture surface from 14-pass, autogenous EBW in uranium (0.625-in. weld penetration) (3X)

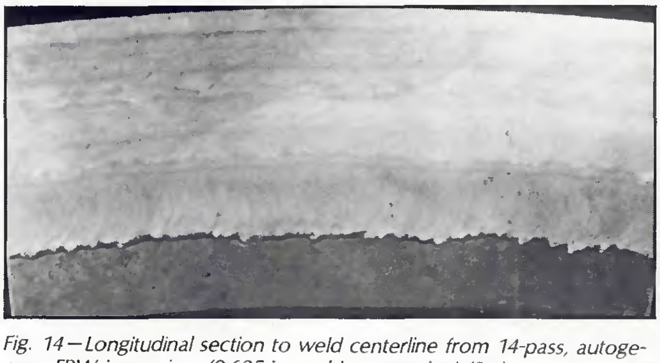

Fig. 14—Longitudinal section to weld centerline from 14-pass, autogenous EBW in uranium (0.625-in. weld penetration) (3X)

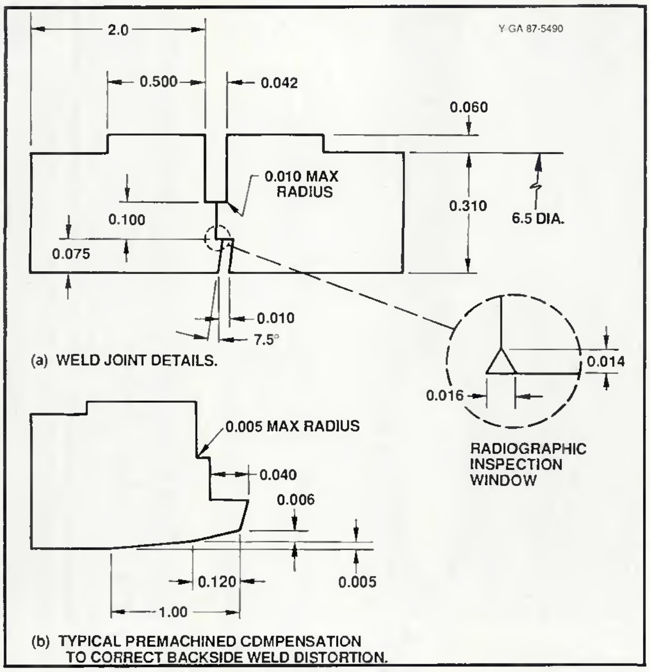

Fig. 15 — Weld joint geometry for multipass, autogenous EB welding of aluminum (Dimensions in in.)

did not consider the effects of the overlap encountered when welding a cylindrical section. Because of concerns with the loss of magnesium from the 5083 alloy during EB welding, it was decided to conduct the study using three different methods of joint filling after the autogenous EB root pass. The EB root pass was chosen as a method to minimize distortion and allow the sealing of containers under vacuum. The fill methods evaluated were: 1) multipass, autogenous EB fill, 2) cold wire-fed EB fill, and 3) gas metal arc (GMA) fill.

The joint geometry that was selected for multipass autogenous electron beam fill is shown in Fig. 15. This joint has a root face of 0.100 in. (2.54 mm) which was selected as a depth that could be consistently welded without melting through the alignment step. This root penetration is 57%, safely within the guidelines of Weidner and Shuler (Ref. 7). The groove and weld boss dimensions were established first by volume calculation and then revised slightly after preliminary welds were made and evaluated. The 0.060-in. (1.5-mm) high weld boss is removed subsequent to the welding. A cross-section of an EB root bead is shown in Fig. 16. The cylinders were machined from aluminum alloy pipe which did not have a uniform metallurgical structure. The variation, which is evident in the figures, had no adverse effect on weldability. The multipass autogenous EB fill beads (Fig. 17) were made by oscillating the electron beam (see Table 4) transverse to the weld joint.

In the multipass, autogenous process, the second, or fill, pass weld melts the groove of the joint and penetrates an adequate depth into the root bead. An early attempt to multipass weld aluminum using techniques that were developed for uranium was not successful. The physical characteristics of aluminum, including density and surface tension, made it difficult for shallow liquid weld metal to readily flow in a groove. It was necessary to melt the entire groove, which had a width of approximately 0.033 in. (0.84 mm), subsequent to completion of the root pass. The third, or cover, pass washes more base metal into the weld and improves the total fill. Backside weld contour was controlled by a premachined compensation (Fig. 15) as had been done for the earlier uranium weld — Fig. 4. The 7.5-deg bevel angle on the alignment step is again used to lock the mating steps together to prevent misalignment.

For the cold wire-fed EB welds, the autogenous root pass was followed by three wire-fed passes using the joint

Table 4—Welding Parameters for Multipass, Autogenous EB Welding of Aluminum Alloy 5083

Weld Pass(a)	Beam Current (mA)	Weld Speed (ipm)	Beam Focus(b) (mA)	Beam Oscillation(c) (in.)
1	9.3	40	495	None
2	17.0	40	520	0.080
3	17.0	40	520	0.080
4	17.0	40	540	0.080

(a) A ribbon filament gun was used. Voltage was constant at 120 kV.
(b) Sharp focus at the root of the joint was 470 mA at a heat shield-to-work distance of 10.6 in. and a beam current value of 2 mA.
(c) The electron beam was oscillated transverse to the weld joint (X-direction) at 1 kHz to the dimension shown.

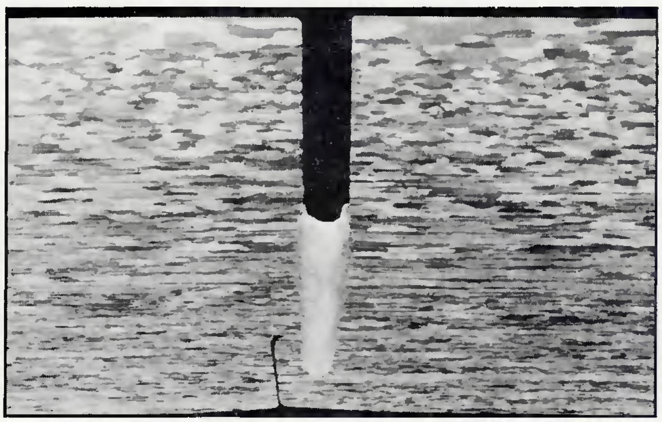

Fig. 16 — Cross-section from an EB root bead in aluminum Alloy 5083 (10X)

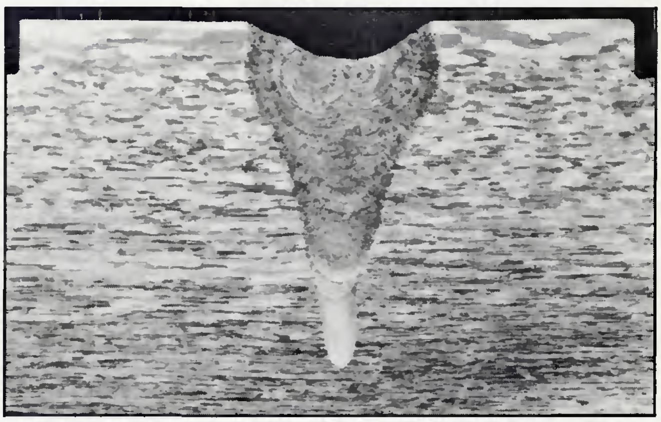

Fig. 17 — Cross-section from a 3-pass, autogenous EBW in aluminum Alloy 5083. D/W ratio is 1.8/1 (weld boss not removed) (8X)

geometry shown in Fig. 18. A cross-section of a weld is shown in Fig. 19. The porosity in this figure is less than 0.004 in. (0.1 mm) in diameter.

The GMA filled welds used the joint geometry shown in Fig. 20. This joint utilized a root face of 0.060 in. for the EB weld. Aluminum Alloy 4043 filler wire was used for the three GMA fill passes. It was realized that 4043 is not an alloy recommended for welding high-magnesium alloys due to the production of Mg_2Si in the weld metal which reduces weld ductility (Ref. 13). It was, however, available at the welding station, and it was felt that it would give adequate information on weld distortion. The weld in Fig. 21 was made using the welding parameters listed in Table 6. Longitudinal beam deflection combined with defocus produced wider root beads for the GMA and cold wire-fed EB processes compared to the multipass, autogenous process which used only a defocused beam – Tables 4-6.

In the comparison of aluminum welds, one of the primary concerns with EB welding of aluminum-magnesium alloys is the loss of alloying additions from the weld, especially magnesium, due to selective evaporation in the high-vacuum environment. Each of the three welding processes was, therefore, checked for magnesium content. The GMA weld was also checked for silicon concentration as a 5 wt-% silicon alloy filler wire was used. The weld metal composition was determined by electron microprobe starting at the top of the weld and taking a measurement every 0.01 in. (0.25 mm) down the centerline of the weld cross-section. The data (Fig. 22) show that the loss of magnesium from the autogenous root beads was 0.6 to 1.1 wt-%. This compares well with the findings of Weidner and Shuler (Ref. 7) that 15 to 25% of the original magnesium content is lost during EB welding. A loss was also seen in the second and third autogenous EB weld beads to make a total loss of 1.1 wt-%. The increased loss (0.5 wt-%) in the third pass was due to the larger surface-to-volume ratio of this wide, shallow, cover pass. The extreme loss of magnesium from the third pass of the cold wire-fed weld would indicate an almost complete loss of magnesium from the 5 wt-% filler wire (aluminum Alloy 5356). The relationship of the silicon and magnesium concentrations shown in Fig. 22 gives a relative measure of the dilution of the base metal with the filler metal alloy (4043) at the various levels in the GMA weld.

Table 5—Welding Parameters for Autogenous EB Root Weld and Cold Wire-Fed Fill Welding of Aluminum Alloy 5083

Weld Pass[a]	Beam Current (mA)	Weld Speed (ipm)	Beam Focus[b] (mA)	Beam Oscillation[c]	Wire Feed Rate[d] (ipm)
1	11	40	500	(0.100 in.) Y	None
2,3,4	13	7.04	510	(0.080 in.) X	45.0

(a) A ribbon filament gun was used. Voltage was constant at 120 kV.
(b) Sharp focus at the root of the joint was 470 mA at a beam current value of 2 mA and at a heat shield-to-work distance of 10.6 in.
(c) The electron beam was oscillated longitudinal (Y-direction) or transverse (X-direction) at 1 kHz to the dimension shown.
(d) Aluminum Alloy 5356 wire was 0.035 in. in diameter.

Table 6—Welding Parameters for EB Root Weld and Gas Metal Arc Fill Welding of Aluminum Alloy 5083

Autogenous EB Root Weld

Weld Pass[a]	Beam Voltage (kV)	Beam Current (mA)	Weld Speed (ipm)	Beam Focus[b] (mA)	Oscillation[c] (in.)
1	120	9.5	40	500	0.100

GMAW

Weld Pass[d]	Volts	Current (A)	Speed (ipm)	Feed Rate[e] (ipm)
2	24	170	80	714
3	26.5	170	80	714
4	29	170	80	714

(a) A ribbon filament gun was used.
(b) Sharp focus at the root of the joint was 470 mA.
(c) The electron beam was oscillated longitudinal to the weld joint (Y-direction) at 1 kHz to the dimension shown.
(d) A cover gas mixture comprising argon and helium was used.
(e) Aluminum Alloy 4043 wire (0.030 in.).

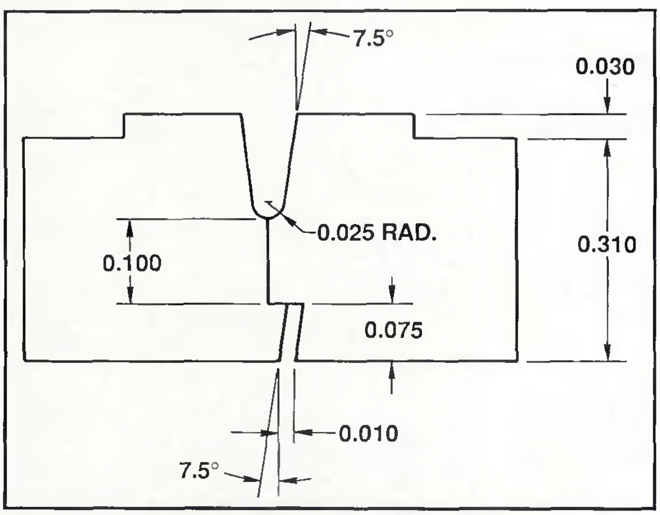

Fig. 18 – Weld joint geometry for autogenous EB root bead and cold wire-fed EB fill (Dimensions in in.)

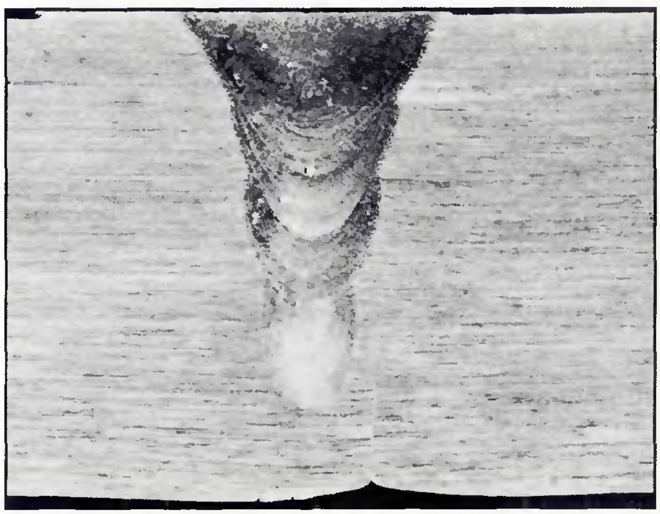

Fig. 19 – Cross-section from autogenous EB root bead and three cold wire-fed EB fill beads in aluminum Alloy 5083 with 5356 filler wire. D/W ratio is 1.5/1 (weld boss removed) (8X)

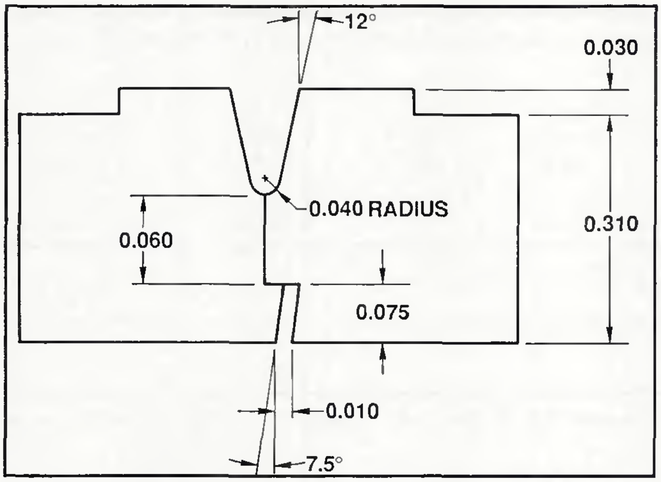

Fig. 20 — Joint geometry for autogenous EB root bead and gas metal arc fill beads (Dimensions in in.)

Fig. 21 — Cross-section from autogenous EB root bead and three GMA fill beads in aluminum Alloy 5083 with aluminum Alloy 4043 filler wire. D/W ratio is 1/1 (weld boss removed) (10X)

The average mechanical properties of the three welds are given in Table 7. The specimen used to determine these properties included a full joint cross-section with the weld boss removed. There was, therefore, a notch present at the weld root due to the alignment step. These data show that there is no significant difference in the strengths of the welds. The ultimate strength is, however, lower than would have been expected from a GMA weld made with a matching filler metal such as aluminum Alloy 5356. In that case, an ultimate strength of 41 ksi (280 MPa) would have been expected (Ref. 14). The notch in the specimen design is probably responsible for this reduced strength. The reduction in magnesium in the weld metal is a less likely cause of this loss of strength as the failures were located in the weld heat-affected zone. Similarly, the elongations are below the 13.6% that would have been expected from such a GMA weld (Ref. 14). This may be due to the narrowness of the EB welds, which causes the majority of deformation to occur in a small portion of the gauge length.

The multipass, autogenous EB and the GMA welding processes resulted in approximately the same dimensional distortion in the cylinders — Table 8. The cold wire-fed EB welding process resulted in the highest distortion. This is due to the high heat input and low welding speed used for the wire-fed process. This low speed was necessary to adequately control the wire-feeding equipment.

Radiography was used to determine the amount of porosity in the various welds. Those that were made by the EB processes had approximately the same level of porosity (less than five pores per inch of weld), while the GMA welds had

Table 7—Comparison of Mechanical Properties of Welds

	Multipass Autogenous Electron Beam	Cold Wire-Fed Electron Beam	Gas Metal Arc
Tensile strength (ksi)	37.8	36.4	38.7
Yield strength (ksi) 0.2% O.S.	21.6	21.6	22.4
Elongation (%)	9.6	11.2	6.7

Table 8—Comparison of Transverse and Diametrical Distortion in Welded Cylinders

	Weld Process		
	Multipass Autogenous Electron Beam	Cold Wire-Fed Electron Beam	Gas Metal Arc
Total weld passes	4	4	4
Average transverse shrinkage (in.)	0.022	0.031	0.022
Diametrical distortion (in.)	0.012–0.75[a]	0.040–1.0[a]	0.013–1.0[a]
Welding speed of fill welds (ipm)	40.0	20.0	80.0

(a) Distortion measurement applies to both sides of the base metal. Distortion was maximum immediately under the weld and minimum at the distance from the weld that is indicated.

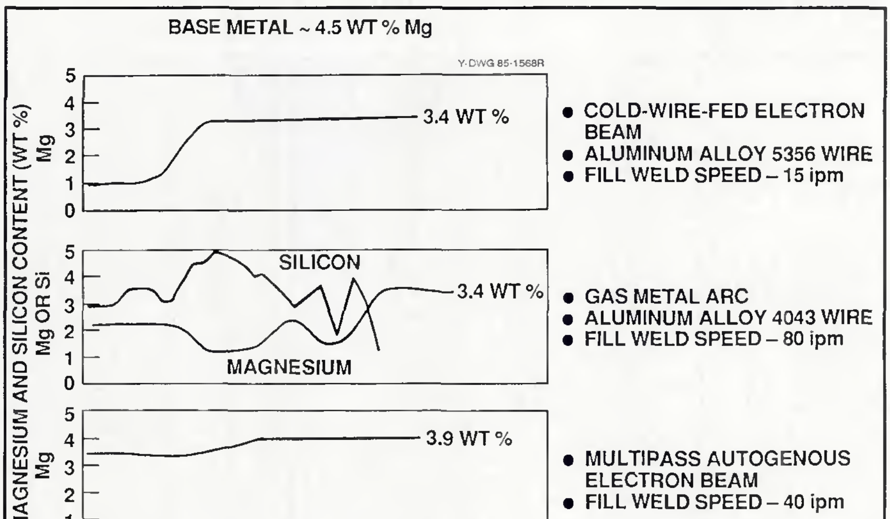

Fig. 22 — Weight-percent magnesium and silicon content in welds in aluminum Alloy 5083

numerous pores. A radiographic window was also used to verify weld penetration. The triangular window is shown in Fig. 15. An acceptable weld would melt-out this window so that it would not be visible during radiographic inspection. An ultrasonic window has also been developed for use with multipass welds in aluminum.

Conclusions

Multipass, autogenous EB welding is established as a method to achieve high quality, deep penetration welds in uranium and aluminum Alloy 5083. The process has been shown to eliminate cold shuts in uranium welds and to provide closely controlled penetration.

Multipass, autogenous EB welds maintain the characteristic high depth-to-width ratios and low heat input of single-pass EB welds. It has been shown that the increased part distortion of multipass welds over single-pass EB welds can be corrected by a preweld machined compensation. The distortion of multipass, autogenous welds is still less than that of arc welds. Multipass, autogenous EB welds have mechanical properties which compare well with single-pass EB welds or arc welds in these materials. Parameter changes that are necessary in multipass welding can be done manually with a check-off procedure and a stop watch or part revolution/degree counter. Computer control of the welding parameters is advantageous.

Acknowledgments

The authors thank E. Luttrell and B. G. Cross for producing the experimental welds. Appreciation is extended to the Y-12 Development Division management for their support and permission to publish this work, and in particular R. A. Huber for his review of the manuscript. The developments described in this paper were sponsored by the United States Department of Energy under contract with Martin Marietta Energy Systems, Inc.

References

1. Hicken, G. K., and Booco, W. G. 1968. Penetration variations in electron beam welding. *Third International Conference on Electron and Ion Beam Science and Technology*, John Wiley and Sons, Inc., New York, N.Y., p. 398.
2. Huber, R. A., and Turner, P. W. 1969. Electron beam welding at the Oak Ridge Y-12 Plant. *Welding Journal* 48(10):787–799.
3. Sandstrom, D. J., Buchen, J. F., and Hanks, G. S. 1970. On the measurement and interpretation and application of parameters important to electron beam welding. *Welding Journal* 49(7):293-s to 300-s.
4. Armstrong, R. E. 1970. Control of spiking in partial penetration electron beam welds. *Welding Journal* 49(8):282-s to 288-s.
5. Bradburn, E. H., Huber, R. A., and Turner, P. W. 1971. Multipass electron beam welding for controlled penetration. *Welding Journal* 50(4):190-s to 193-s.
6. Weber, C. M., Funk, E. R., and McMaster, R. C. 1972. Penetration mechanism of partial penetration electron beam welding. *Welding Journal* 51(2):90-s to 94-s.
7. Weidner, C. W., and Shuler, L. E. 1973. Effect of process variables on partial penetration electron beam welding. *Welding Journal* 52(3):114-s to 119-s.
8. Mara, G. L., Funk, E. R., McMaster, R. C., and Pence, P. E. 1974. Penetration mechanisms of electron beam welding and the spiking phenomenon. *Welding Journal* 53(6):246-s to 251-s.
9. Murphy, J. L., and Turner, P. W. 1976. Wire feeder and positioner for narrow groove electron beam welding. *Welding Journal* 55(3):181–190.
10. Bench, F. K., and Ellison, G. W. 1974. EB welding of 304L stainless steel with cold wire feed. *Welding Journal* 53(12):763–770.
11. Wood, D. H., and Mara, G. L. 1977. Eliminating cold shut defects in deep, single pass, electron beam welds in uranium. *Welding Journal* 56(3):88-s to 92-s.
12. Moyer, *et al.* Ultrasonic inspection of uranium welds with a step geometry. To be published.
13. Dudas, J. H., and Collins, F. R. 1966. Preventing weld cracks in high-strength aluminum alloys. *Welding Journal* 45(6):241-s to 249-s.
14. Liptak, J. A., and Baysinger, F. R. 1968. Welding dissimilar aluminum alloys. *Welding Journal* 47(4):173-s to 180-s.